NASA TECHNICAL REPORT

NASA TR R-196

NASA TR R-196

DETERMINATION OF EFFECTS OF OXIDATION ON PERFORMANCE OF CHARRING ABLATORS

by Marvin B. Dow and Robert T. Swann

Langley Research Center
Langley Station, Hampton, Va.

NATIONAL AERONAUTICS AND SPACE ADMINISTRATION • WASHINGTON, D. C. • JUNE 1964

DETERMINATION OF EFFECTS OF OXIDATION ON PERFORMANCE OF CHARRING ABLATORS

By Marvin B. Dow and Robert T. Swann

Langley Research Center
Langley Station, Hampton, Va.

NATIONAL AERONAUTICS AND SPACE ADMINISTRATION

For sale by the Office of Technical Services, Department of Commerce,
Washington, D.C. 20230 -- Price $1.00

DETERMINATION OF EFFECTS OF OXIDATION ON PERFORMANCE OF CHARRING ABLATORS

By Marvin B. Dow and Robert T. Swann
Langley Research Center

SUMMARY

An investigation of phenolic-nylon specimens was conducted in an atmospheric-pressure subsonic electric-arc-powered jet using gas streams of nitrogen and different oxygen concentrations. No char removal was observed for specimens tested in nitrogen; therefore, oxidation appears to be the only mechanism of char removal for these specimens. With sufficiently high heating rates and low total heat input, the results can be correlated in terms of a diffusion limited mechanism. The results of tests with larger total heat input are discussed.

A surface energy balance of the heat input and of the heat accommodated by various mechanisms is calculated. With oxygen concentrations of 11.5 percent and higher, it was found that the heat input resulting from combustion is a significant part of the total heat input.

The effectiveness of a charring ablator as determined by the time required to achieve a certain back surface temperature rise is strongly influenced by the oxygen concentration in the test stream. The effectiveness of phenolic nylon tested in nitrogen is more than 70 percent higher than the effectiveness of the same material tested in air.

INTRODUCTION

Vehicles entering the earth's atmosphere at high velocities are subjected to severe heating. A number of methods are available for protecting the interior of a reentering spacecraft. In general, charring ablators, subliming ablators, and melting ablators provide the most effective thermal-protection systems. Of these, the charring ablator is superior for a wide range of applications, including the stagnation area of manned reentry vehicles.

The performance of a charring ablator at the stagnation point of a vehicle entering the earth's atmosphere at hyperbolic velocity is analyzed in reference 1. The principal difficulty encountered in such an analysis is the lack of knowledge concerning the mechanism of char removal. The mechanisms of char removal postulated in reference 1 are shear and thermal stresses, internal or external pressure, and oxidation.

Removal of char as a result of internal pressure has been investigated analytically. (See ref. 2.) The results of this study indicate that for some materials the char will build up to a certain thickness and then be blown off by the internal pressure and thermal stresses. Studies of the removal of char by aerodynamic shear are not available. Results of a detailed experimental study of char formation and removal are presented in reference 1. The tests were conducted in a subsonic atmospheric-pressure electric-arc-powered jet. Under these conditions, for the material tested the general feature of char removal as a result of internal pressure was not observed. The analysis of reference 3 indicates that the results of reference 1 are consistent with an oxidation mechanism of char removal which in some instances may be diffusion controlled.

Speculation as to the effects of oxidation on the char formation and removal for the materials tested in the investigation of reference 1 made it desirable to conduct an experimental study of similar materials with the same test facility and control the oxygen concentration of the arc jet.

In the present paper, the results of such a study are presented. Some preliminary results from this study were presented in reference 4. A typical charring ablation material was exposed to a high-temperature arc-jet stream of controlled oxygen content to investigate the effect of oxygen concentration on the material char removal, depth of pyrolysis, surface temperatures, surface energy balance, and ability of a given weight of material to limit back surface temperature rise. Data were obtained from tests in which the oxygen concentration was varied from 0 to 50 percent by weight. Two ranges of convective heat-transfer rate were used in testing, the ranges being 108 to 121 $\frac{\text{Btu}}{\text{ft}^2\text{-sec}}$ and 171 to 193 $\frac{\text{Btu}}{\text{ft}^2\text{-sec}}$. In addition, the results of char removal were correlated in terms of the rate at which oxygen diffuses through the boundary layer to the surface.

SYMBOLS

C concentration of oxygen

$\overline{C} = \frac{C}{C_e}$

E effectiveness, $\frac{\text{Heat input before } 300^\circ \text{ F rise}}{\text{Weight of material}}$

f volatile fraction, $\frac{\rho - \rho_c}{\rho}$

H total enthalpy

$$\overline{H} = \frac{H - H_w}{H_e - H_w}$$

H_a	heat of ablation
Δh	heat absorbed by surface per unit of mass injected into boundary layer
Δh_l	heat of combustion per unit weight of char
$\dot{m}$	rate of mass transfer into boundary layer
$\dot{m}_c$	rate of char removal
$\dot{m}(O_2)$	rate at which oxygen diffuses to surface
$\dot{m}_p$	rate of formation of gaseous products of pyrolysis
N_{Le}	Lewis number
N_{Pr}	Prandtl number
N_{Sc}	Schmidt number
Q	integrated heat input
q_c	convective heating rate with mass transfer
$q_{c,o}$	convective heating rate with no mass transfer
q_r	net radiant heating rate
q_l	combustive heating rate
u	velocity in boundary layer parallel to surface
v	velocity in boundary layer normal to surface
W	weight of heat-shield material
x	boundary-layer coordinate parallel to surface
y	boundary-layer coordinate normal to surface
z_c	char thickness
z_p	depth to which pyrolysis has penetrated from initial surface location

η transpiration factor

λ weight of char removed per unit weight of oxygen diffusing to surface

μ viscosity

ρ density

ρ_c char density

ρ' density of boundary-layer fluid

Subscripts:

e condition in flow external to boundary layer

w wall value

TEST MATERIAL AND PROCEDURES

Test Material

The test material was a mixture of equal parts by weight of phenolic resin and powdered nylon with a density of 75 pounds per cubic foot. Test specimens consisting of 3-inch-diameter flat-face cylinders of different thicknesses were machined from large blanks of phenolic nylon.

Prior to testing, the specimens were attached to a brass mounting ring as shown in figure 1. The specimens used in determining the ability of the material to limit back surface temperature rise were instrumented as shown in figure 1. The specimens used to determine the effects of oxidation were uninstrumented.

Test Procedures

Tests were performed by exposing the 3-inch-diameter front face of the specimens to the high-temperature gas stream produced by the 2500-kilowatt arc jet at the Langley Research Center. This facility is described in reference 5. It produces a subsonic gas stream at atmospheric pressure having a static temperature of about 6,400° F and a constant enthalpy of approximately 3,000 Btu/lb. The photograph of figure 2(a) shows the arc-jet facility with a specimen in the test position.

The specimens were attached to the water-cooled sting of a movable inserter (fig. 2(a)) by means of the brass holders shown in figure 1. The removable inserter positioned the specimen after the arc jet had been started and the proper operating conditions had been established. All specimens were tested with the front face initially a distance of 2 inches from the top edge of the nozzle. Measurements of the "cold-wall" heat-transfer rate were made immediately before

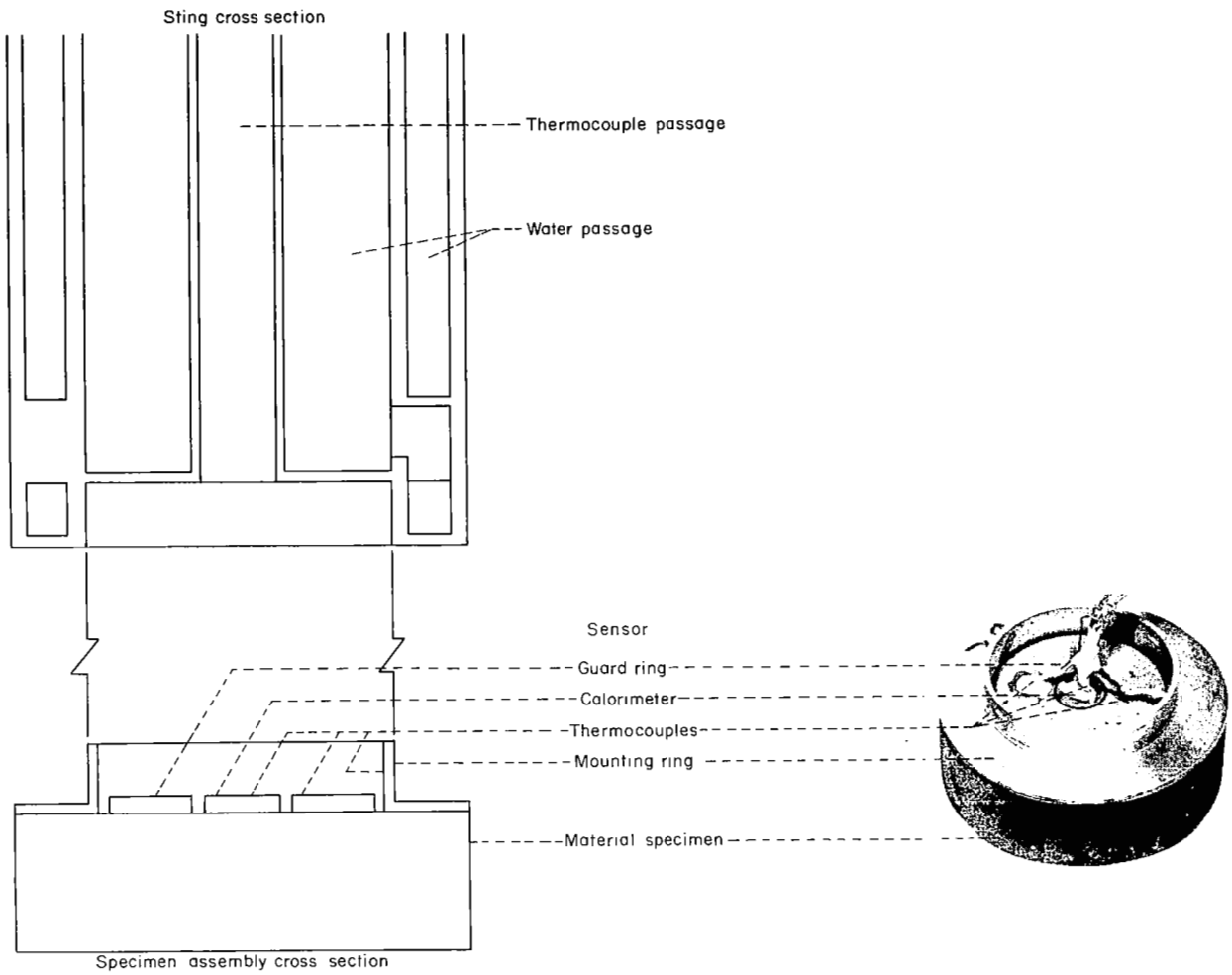

L-64-351

Figure 1.- Instrumented test specimen showing brass mounting ring and instrumentation.

and after specimen exposure by means of a 3/8-inch-diameter water-cooled heat-transfer-rate probe shown in figure 2(a). Construction details and operation of the probe are described in reference 5. The heat-transfer rates measured by the probe were adjusted to give the heat-transfer rates at the stagnation point of the 3-inch-diameter specimens by means of an experimentally determined correction factor.

The free-stream temperature of the jet was measured at a height of 2 inches above the nozzle. The temperature was measured spectrographically by an atomic-line-intensity ratio method by using the electronic excitation spectrum of copper that appears in the gas caused by the small contamination from the arc-jet electrodes. This temperature-measuring technique is discussed in detail in reference 6. Determinations of the stream temperature were made before and after specimen exposure.

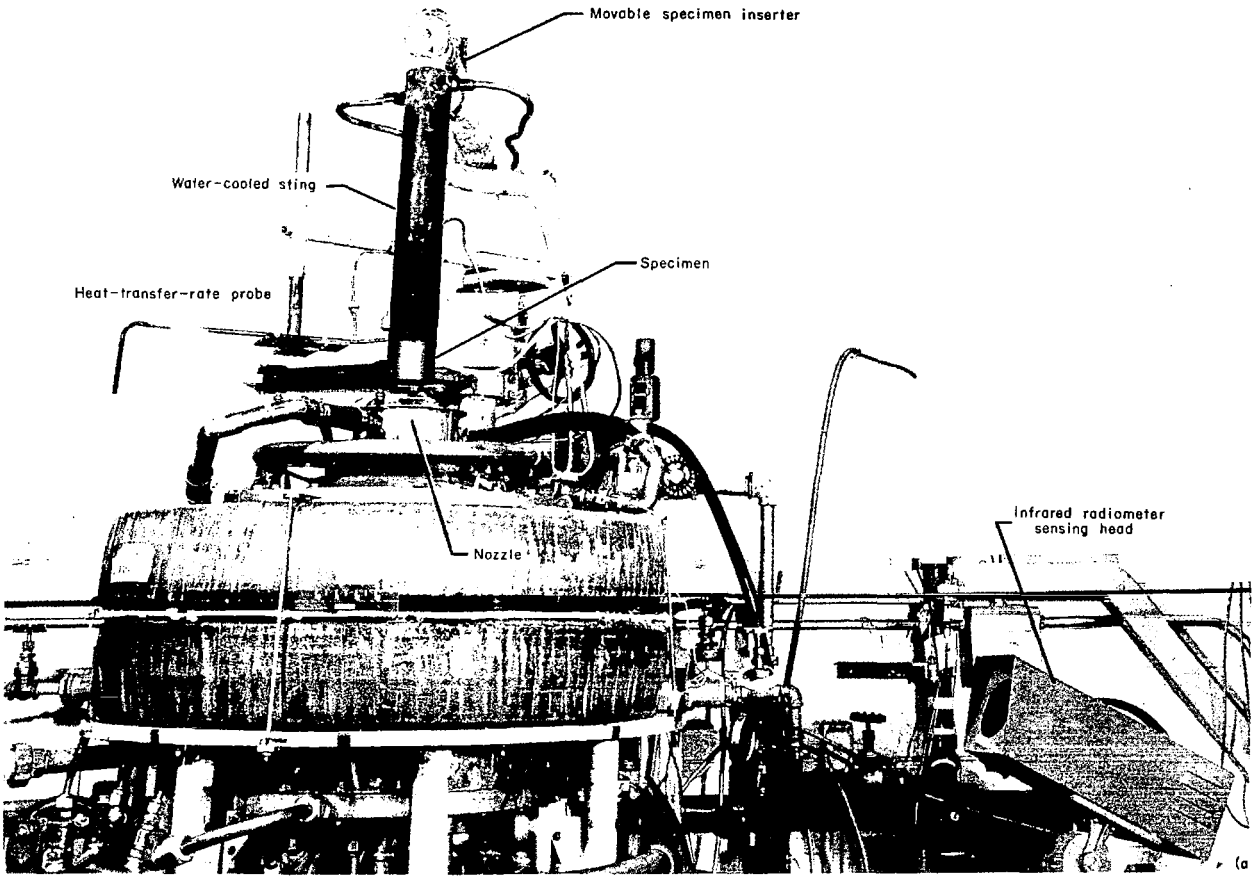

(a) Arc-jet test setup. L-64-352

Figure 2.- Test facility.

During testing, a continuous record of specimen surface emission was obtained for some of the specimens through the use of an infrared radiometer. The sensing head of this instrument, as shown in figure 2(a), was focused on the stagnation point of the specimen surface as close to the vertical as possible in order to minimize the effect of the target displacement due to specimen surface regression.

To allow testing in an arc-jet stream with controlled oxygen content, the normal air supply for the arc jet was modified to permit operation with varying percentages of oxygen and nitrogen. The gas supply system and the instrumentation for controlling and measuring the flow of gases to the arc jet are shown schematically in figure 2(b). The mass flow rate of gas (0.35 pound per second) was the same for all tests regardless of gas composition.

Two ranges of heat-transfer rate were obtained by using a 2-inch- or a 4-inch-diameter nozzle. The gas stream from the 2-inch-diameter nozzle had a

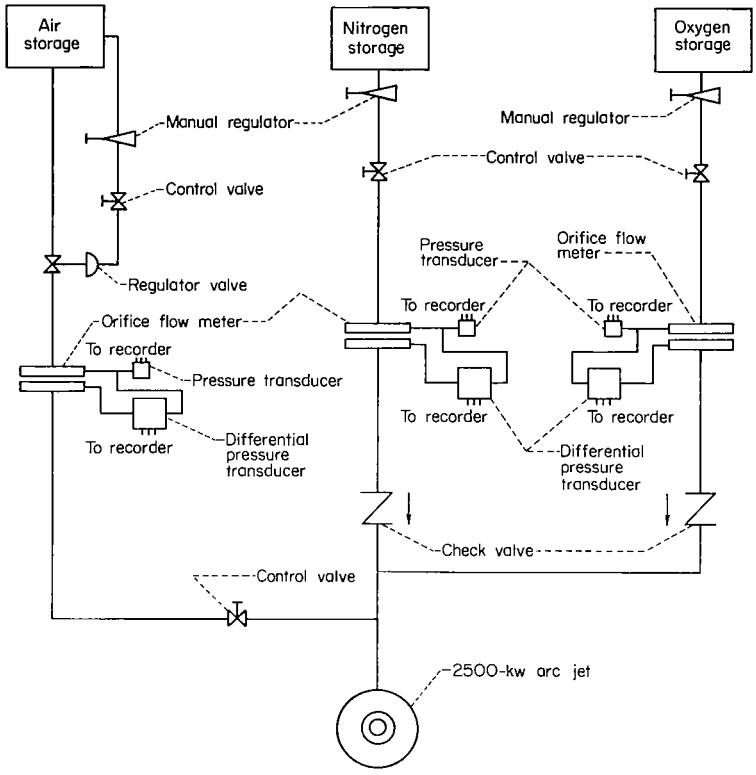

(b) Gas supply system.

Figure 2.- Concluded.

velocity of approximately 3,400 feet per second and produced cold-wall heat-transfer rates of 171 $\frac{\text{Btu}}{\text{ft}^2\text{-sec}}$ to 193 $\frac{\text{Btu}}{\text{ft}^2\text{-sec}}$. Tests of the 3-inch-diameter specimens in the gas stream from this nozzle were of the "splash" type in which the hot gas heats the specimen front surface but is deflected away from the sides so that very little heating occurs on the specimen sides. The gas stream from the 4-inch-diameter nozzle had a velocity of approximately 850 feet per second and produced cold-wall heat-transfer rates of 108 $\frac{\text{Btu}}{\text{ft}^2\text{-sec}}$ to 121 $\frac{\text{Btu}}{\text{ft}^2\text{-sec}}$. Three-inch-diameter specimens tested in the gas stream from this nozzle were immersed in the stream. This immersion resulted in substantial heating on the specimen sides.

The specimens used to determine char-removal rates and pyrolysis depths were exposed to the arc-jet stream for fixed time intervals. After testing, the thickness of material removed at the stagnation point of the specimen was determined by measuring the overall thickness of the specimen and subtracting the measurement from the previously measured thickness of the specimen before testing. The depth of pyrolysis in each specimen was determined from a diametrical section. The distance to the char—virgin-material interface was measured from the back surface of the specimen and the distance was subtracted from the specimen thickness before testing to provide a measure of pyrolysis depth.

The specimens used to determine the ability of the material to limit back surface temperature rise were all of equal thickness and were exposed to the gas stream until the copper calorimeter at the back of the specimen (fig. 1) experienced a temperature rise of 300° F. The time required for the temperature rise to occur was determined from oscillograph recordings. This type of test was conducted only with the 2-inch-diameter nozzle.

ANALYSIS

Char removal by oxidation depends on the reaction rate and on the concentration of oxygen at the surface. For the case in which the reaction rate is high and the oxidation process is controlled by the amount of oxygen diffusing to the surface, it is shown in the appendix that the rate of char removal by oxidation is

$$\dot{m}_c = \frac{\lambda C_e N_{Le}^{0.6}}{1 + \lambda \eta C_e N_{Le}^{0.6}} \left(\frac{q_{c,o}}{H_e - H_w} - \eta \dot{m}_p \right) \tag{1}$$

Equation (1) applies to the case in which all the available oxygen reacts with the char and none reacts with the gaseous products of pyrolysis. The validity of this assumption can be determined only from a detailed aerothermochemical analysis of the boundary layer or from a comparison of experimental results with the result given by equation (1).

The rate at which heat is added to the surface as a result of combustion is

$$q_1 = \dot{m}_c \Delta h_1 \tag{2}$$

where Δh_1 is the heat of combustion per unit weight of char consumed. Since the reaction appears to be a surface reaction, it is assumed in equation (2) that all the heat generated by the oxidation reaction is absorbed by the surface.

RESULTS

The general features of the effect of oxidation on the performance of char-forming ablators are shown in figure 3. The specimens shown in figure 3 were tested under the same conditions except for the oxygen concentration in the arc-jet stream. Since the tests were conducted with the 4-inch arc-jet nozzle, the specimens were immersed in the stream and, as a consequence, experienced considerable heating on the sides. The main point of interest is that specimen 22, which was tested in the absence of oxygen, maintained a completely flat surface, the change in depth probably resulting from shrinkage of the char during formation. The effect of increased oxygen concentration, as evidenced by specimens 16 and 17 of figure 3, is to increase greatly the amount of material removed and to decrease the thickness of the carbonaceous char layer. It would appear from the qualitative differences between the specimens tested in a stream containing only nitrogen and those tested in a stream containing oxygen that char removal occurs only when

(a) Test 22; C_e = 0.

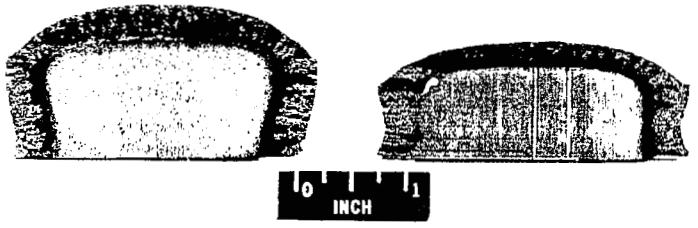

L-62-1013

(b) Test 17; C_e = 0.10. (c) Test 16; C_e = 0.232 (air).

Figure 3.- Effect of oxygen on char removal. Test material, phenolic nylon; heat-transfer rate, 109 to 110 Btu/ft^2-sec; nozzle size, 4 inches; exposure time, 300 seconds. Borders around specimens indicate original specimen size.

there is oxidation. The results of more detailed tests are presented in subsequent sections.

Char Formation and Removal

The results of two investigations of char formation and removal are summarized in table I. The details of the tests in regard to oxygen concentration, heat-transfer rate, and exposure time are also given for each specimen. The test conditions for the two series differ primarily in heating rate; some of the tests were conducted with the 4-inch arc-jet nozzle and some with the 2-inch arc-jet nozzle. Some data are also included from reference 7.

Depth of pyrolysis.- The experimentally measured depths of pyrolysis are shown in figure 4 plotted as functions of total heat input. Definition of the depth to which pyrolysis has penetrated is discussed subsequently. The total heat input is the product of heat-transfer rate and time and thus is proportional to test duration. The curves of figure 4 indicate that the depth of pyrolysis is approximately a linear function of total heat input after a total heat input of about 4,000 Btu/ft^2. The curves of figures 4(a) and 4(b), which present the results of tests with the 4-inch and 2-inch nozzles, respectively, show that the depth of pyrolysis for a given total heat input increased with increasing oxygen concentration. However, a comparison of figures 4(a) and 4(b) shows that the depth of pyrolysis which has occurred with a given total heat input and oxygen concentration is relatively insensitive to heat-transfer rate for the range of values for which a comparison can be made.

Char removal.- The experimentally determined thicknesses of char removed are shown in figure 5 plotted as functions of total heat input. The thickness of char removed is assumed to be equal to the difference between the initial specimen thickness and the thickness of the specimen after testing; that is, the char shrinkage is not considered. Since the amount of char shrinkage is proportional to char thickness, the error involved in this assumption is less than the dimensional changes shown in figure 3(a). Contrary to the results obtained for depth of pyrolysis with a given total heat input and oxygen concentration, the thickness of char removed is greater at the higher heat-transfer rates. (See figs. 5(a) and 5(b).) As shown in figures 5(a) and 5(b), the thickness of char removed increases fairly uniformly with increased total heat input for the two investigations except for the low-oxygen-concentration (C_e = 0.116) tests with the 2-inch

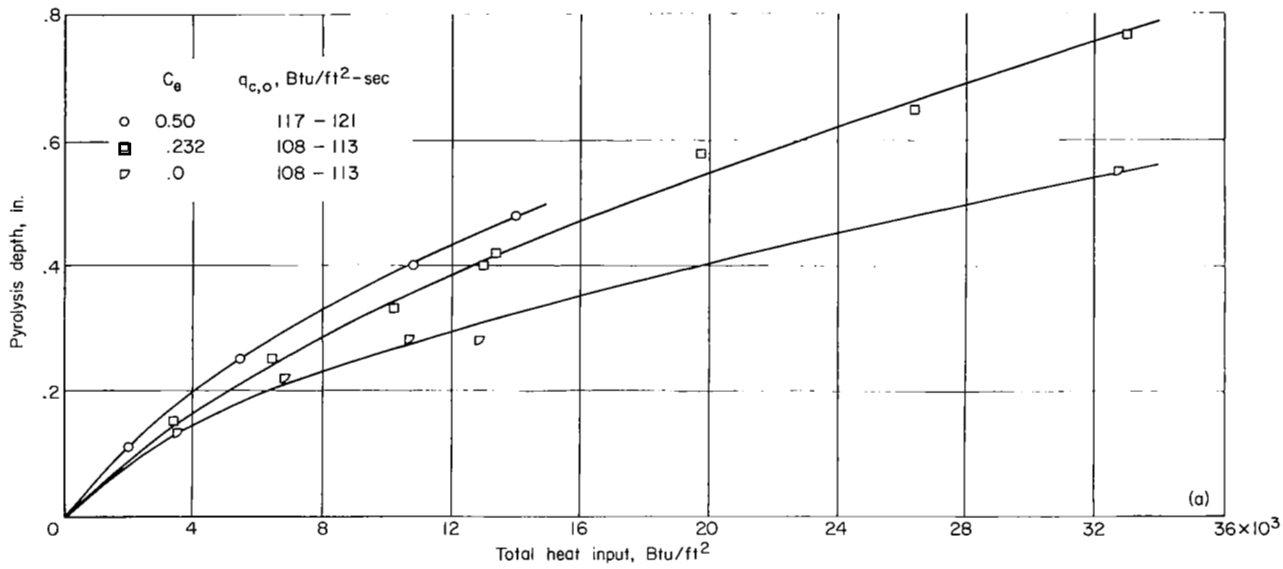

(a) Tests with 4-inch arc-jet nozzle.

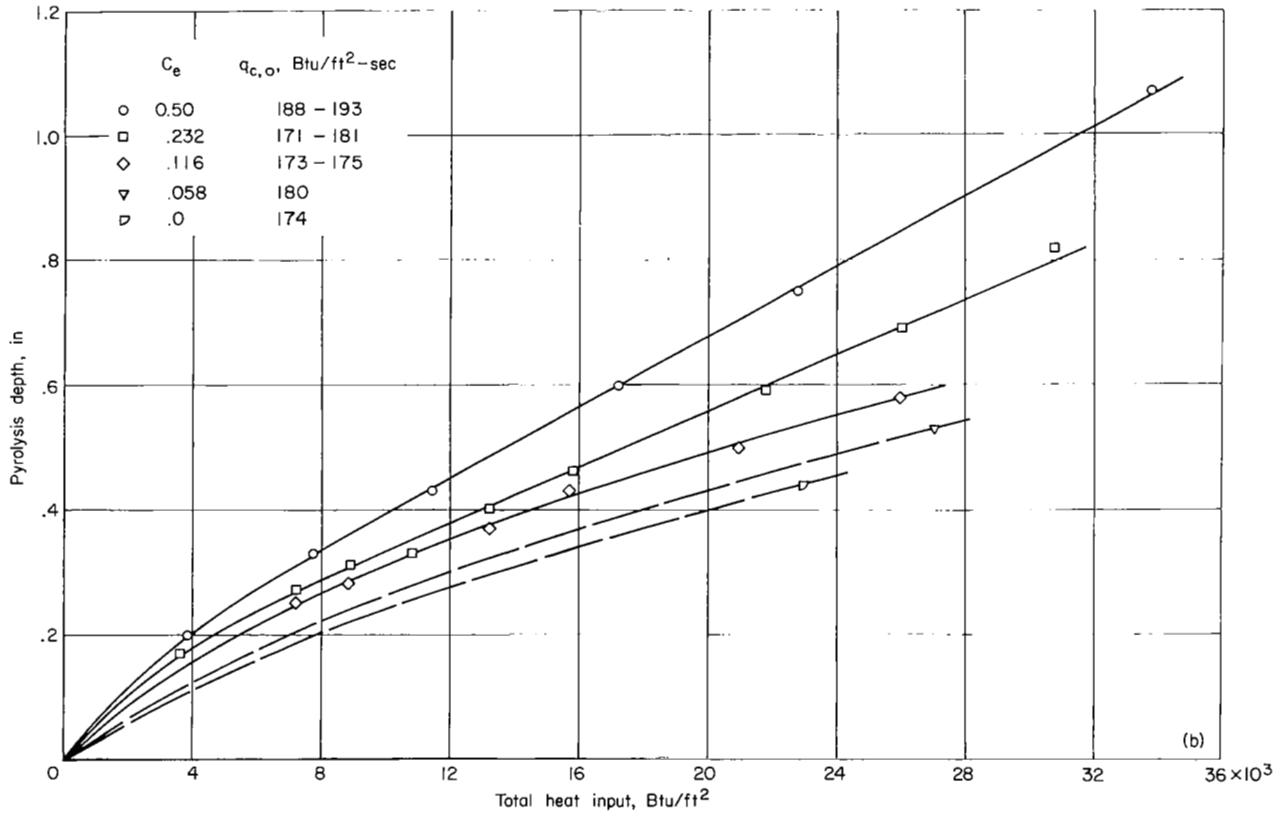

(b) Tests with 2-inch arc-jet nozzle.

Figure 4.- Pyrolysis-depth curves.

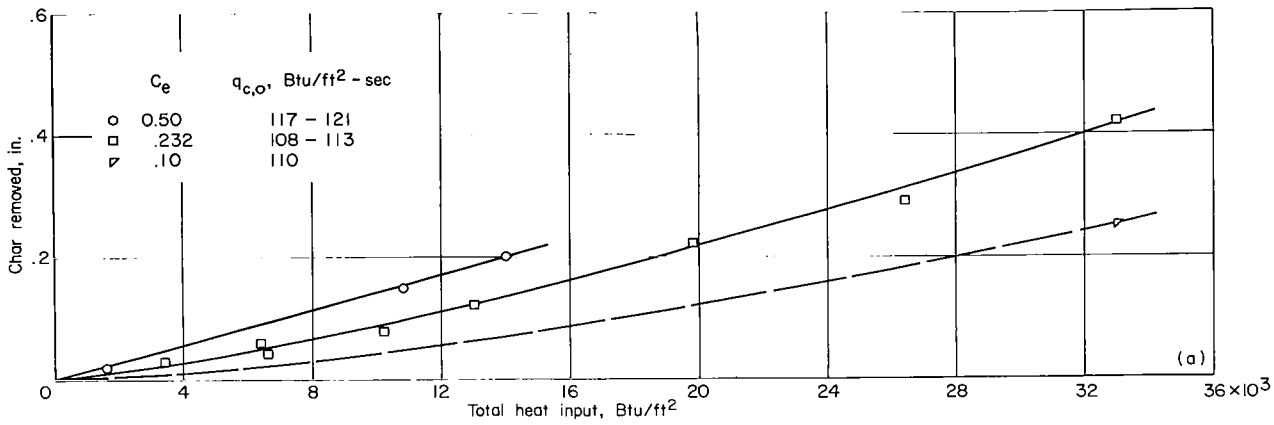

(a) Tests with 4-inch arc-jet nozzle.

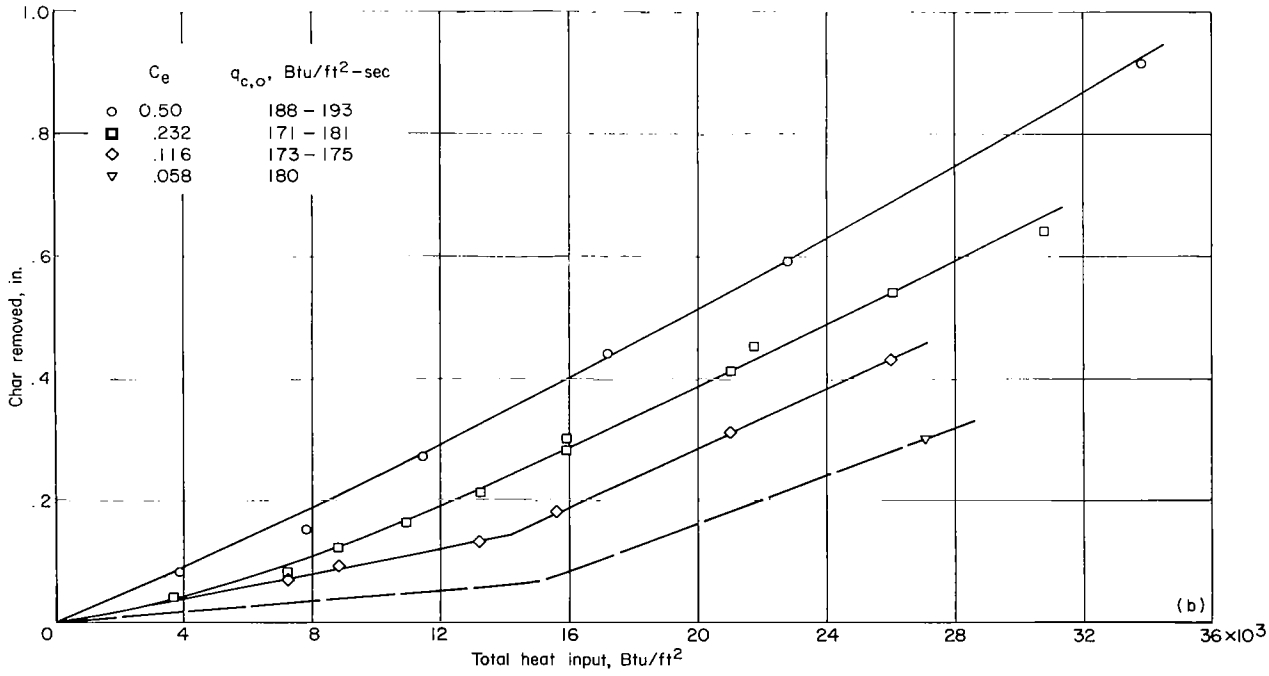

(b) Tests with 2-inch arc-jet nozzle.

Figure 5.- Char-removal curves.

TABLE I.- OXIDATION TESTS

Specimen	Percent O_2 in test gas	Heating rate, Btu/ft^2-sec	Test duration, sec	Char removed, in.	Pyrolysis depth, in.
4-inch-diameter nozzle					
1	50	121	13.5	0.02	0.11
2	50	121	14	.02	.11
3	50	121	45	(a)	.25
4	50	120	90	.15	.40
5	50	117	120	.20	.48
6	23.2	[b]110	31	.03	.15
7	23.2	[b]110	31	(a)	.15
8	23.2	[b]110	60	.04	.25
9	23.2	108	60	.06	.25
10	23.2	113	90	.08	.33
11	23.2	108	120	.12	.40
12	23.2	[b]110	122	.11	.42
13	23.2	[b]110	180	.22	.58
14	23.2	110	180	(a)	.58
15	23.2	[b]110	241	.29	.65
16	23.2	110	300	.42	.77
17	10.0	110	300	.25	.68
18	0	113	31	[c].00	.13
19	0	113	61	[c].02	.22
20	0	113	95	[c].04	.28
21	0	108	120	[c].00	.28
22	0	109	300	[c].07	.55
23	0	117	300	(a)	.55
2-inch-diameter nozzle					
1	50	192	20	0.08	0.20
2	50	193	40	.18	.33
3	50	190	60	.27	.43
4	50	191	90	.44	.60
5	50	190	120	.59	.75
6	50	188	180	.92	1.07
7	23.2	175	21	.04	.17
8	23.2	175	41	.08	.27
9	23.2	174	51	.12	.31
10	23.2	177	61	.16	.33
11	23.2	174	76	.21	.40
12	23.2	174	91	.28	.46
13	23.2	175	91	.29	.45
14	23.2	181	120	.45	.59
15	23.2	174	121	.41	.57
16	23.2	174	150	.54	.69
17	23.2	171	180	.64	.82
18	11.6	180	40	.07	.25
19	11.6	175	50.5	.09	.28
20	11.6	175	75.5	.13	.37
21	11.6	174	90	.18	.43
22	11.6	174	121	.31	.50
23	11.6	173	150.5	.43	.58
24	5.8	180	150.8	.30	.53
25	0	174	132	(a)	.44

[a]Measurement not obtained because of char-layer separation.

[b]Data from reference 7.

[c]Indicates amount of char shrinkage.

nozzle. (See fig. 5(b).) For these tests the rate of char removal increases rather abruptly at a total heat input of about 15,000 Btu/ft^2.

Char thickness.- The difference between the depth of pyrolysis and the thickness of char removed is the char thickness; that is, it is the thickness of char which is available to insulate the unpyrolyzed material from the external environment. In figure 6 the char thickness is plotted as a function of total heat input. Figure 6(a) shows the char thickness produced at the lower heating rate is a monotonic increasing function of total heat inputs to about 20,000 Btu/ft^2. For greater total heat inputs, the available data indicate that the char thickness approaches a constant value for tests in air (C_e = 0.232) and continues to increase for tests in nitrogen (C_e = 0). At the higher heating rate (fig. 6(b)), the char thickness for tests in a high oxygen concentration (C_e = 0.50) quickly reaches a constant value. For the tests at a lower oxygen concentration (C_e = 0.232 and 0.116), the char thickness increases with total heat input until a maximum thickness is reached at a heat input corresponding to the increase in char-removal rate. With further increases in total heat input, the char thickness decreases to the thickness obtained in tests at high oxygen concentration (C_e = 0.50).

Correlation of Char-Removal Rates With a Diffusion Limited Oxidation Mechanism

The experimentally determined thickness of char removed has been plotted in figure 5 as a function of total heat input. From equation (1) it is found that the slope of this curve is

$$\frac{dz_c}{dQ} = \frac{\lambda C_e N_{Le}^{0.6}}{1 - f + \lambda\eta C_e N_{Le}^{0.6}\left[1 - f\left(1 - \frac{dz_p}{dz_c}\right)\right]}\left[\frac{1}{\rho\left(H_e - H_w\right)}\right] \tag{3a}$$

if the char is removed as a result of a diffusion limited oxidation mechanism. If the linear rates of pyrolysis and of char removal are assumed to be equal, equation (3a) can be written as

$$\frac{dz_c}{dQ} = \frac{\lambda C_e N_{Le}^{0.6}}{1 - f + \lambda\eta C_e N_{Le}^{0.6}}\left[\frac{1}{\rho\left(H_e - H_w\right)}\right] \tag{3b}$$

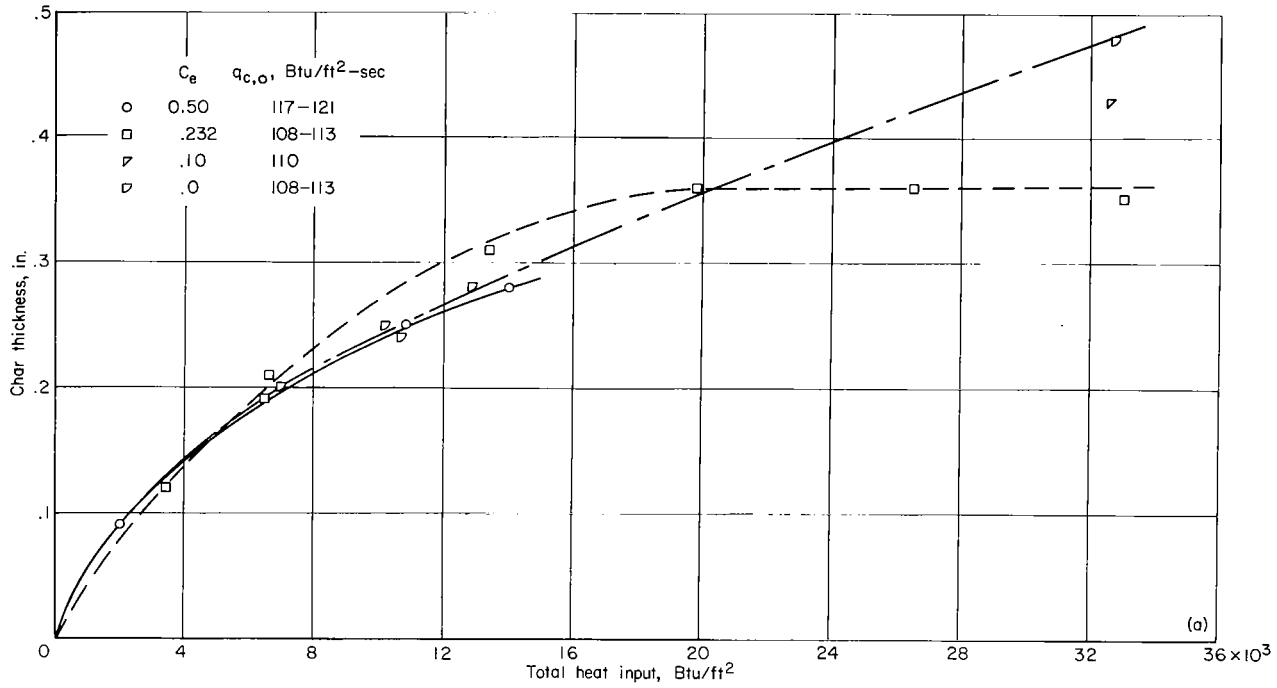

(a) Tests with 4-inch arc-jet nozzle.

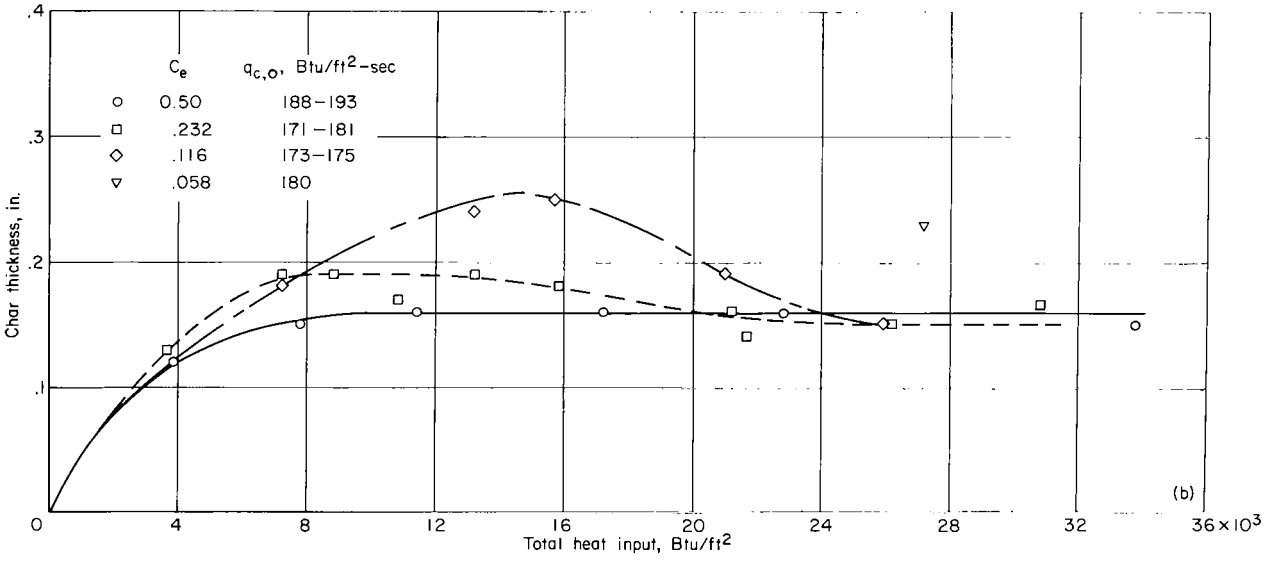

(b) Tests with 2-inch arc-jet nozzle.

Figure 6.- Char-thickness curves.

The errors involved in this assumption are discussed later. The values of C_e and $H_e - H_w$ were determined for each test as part of the test procedure. The density of the original material ρ is known and it has been assumed that the value of λ is 3/4 for diffusion limited oxidation. (See appendix.) Before values of the slope can be calculated from equation (3b), η, f, and N_{Le} must be evaluated.

The value of the transpiration coefficient η depends on the molecular weight of the injected gases and on the character of the boundary-layer flow. It has been experimentally determined that for Teflon the value of η is approximately 0.42 for laminar flow and 0.19 for turbulent flow. (See refs. 8 and 9.) It was determined that with the 2-inch nozzle the transpiration factor for Teflon has a value corresponding to that for turbulent flow. In a similar test with the 4-inch nozzle, the transpiration factor was found to be between the value for laminar flow and the value for turbulent flow. Such turbulence might arise from the a-c arc and might exist in the viscid flow. No determination of the composition of the injected gases was made. However, mass transfer is relatively ineffective in blocking aerodynamic heating in turbulent flow and a value $\eta = 0.2$ was used. This value corresponds to air injection in turbulent flow. The Lewis number was assumed to be unity.

The appropriate value of f depends on the char density at the surface. The char layer is relatively thin and fragile, and it has not been possible to obtain values of the density except for averages through the entire char thickness. In most cases, the average specific gravity of the material in the char layer was 0.485 although in certain cases discussed subsequently the specific gravity was 0.43. When the specific gravity of the char is equal to 0.485, the value of f is 0.60.

The blocking of heat input which is achieved by the gases transpired into the boundary is a relatively small factor in these tests because of the turbulent flow conditions mentioned previously. Likewise the effect of mass transfer on the quantity of oxygen diffusing to the surface is small. Examination of equation (3a) shows that for the existing test conditions, large changes in the ratio of the rate of pyrolysis to the rate of char removal have little effect on the value for dz_c/dQ; therefore, the assumption of a quasi-steady condition as represented by equation (3b) cannot introduce a large error.

The experimental data from figure 5 have been replotted in figure 7 and straight lines having the slopes given by equation (3b) have been fitted to the data. The calculated char removal and experimental char removal at the lower heating rates (108 to 121 Btu/ft^2-sec) as shown in figure 7(a) do not agree, particularly for the tests with high oxygen concentration ($C_e = 0.50$). It appears that a diffusion controlled char-removal condition was not produced in these tests, probably because the test heating rates were too low to produce surface temperatures high enough to provide the reaction rates required to obtain a diffusion controlled condition. That is, there was more oxygen available at the surface than was being consumed in the reactions and the process is rate controlled.

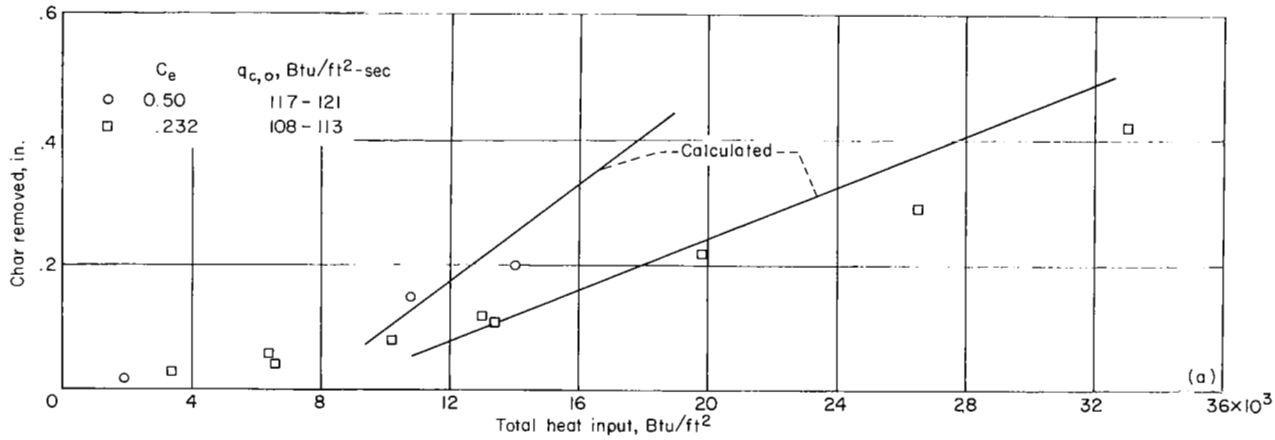

(a) 4-inch arc-jet nozzle.

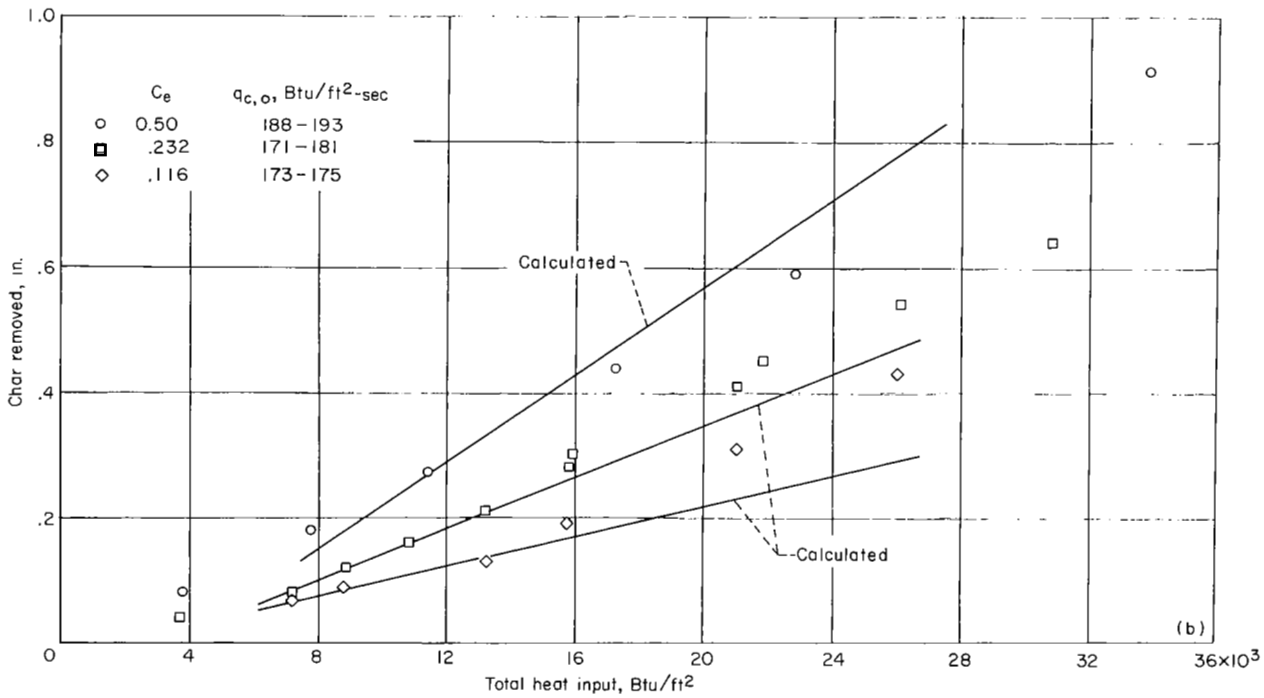

(b) 2-inch arc-jet nozzle.

Figure 7.- Comparison of measured and calculated char removal.

The comparison between calculated char removal and experimental char removal at higher heating rates (171 to 193 Btu/ft^2-sec) is shown in figure 7(b). For the tests at high oxygen content (C_e = 0.50), the char removal again does not appear to be diffusion controlled but rather rate controlled. The calculated and experimental char removal for the lower oxygen concentration tests (C_e = 0.232 and 0.116) show good agreement at the lower total heat inputs up to about 16,000 Btu/ft^2. At higher heat inputs the experimental rate of char removal is significantly higher than predicted, particularly for the lowest oxygen concentration (C_e = 0.116). Although the experimental results indicate that char removal in the test facility is a mechanism of oxidation, it is difficult to reconcile this condition with rates of char removal greater than those predicted on the basis of a diffusion controlled reaction. Factors such as changes in the character of the heating and changes in char density must be considered. These factors are discussed in more detail subsequently.

Surface Temperature Histories

Surface temperature histories are shown in figure 8. The 2-inch-diameter arc-jet nozzle was used in these tests. In general, the temperature is higher with higher oxygen concentration in the test stream. With oxygen in the test stream the surface of the specimen recedes and the area viewed by the radiometer moves from the stagnation point toward the edge of the specimen which is at a higher temperature than the stagnation point. This condition accounts for the erratic temperature measurements at longer times. Significant dimensional changes occur more slowly for the specimens tested in nitrogen; this temperature measurement does not become erratic until char shrinkage causes the area viewed by the radiometer to move toward the edge of the specimen.

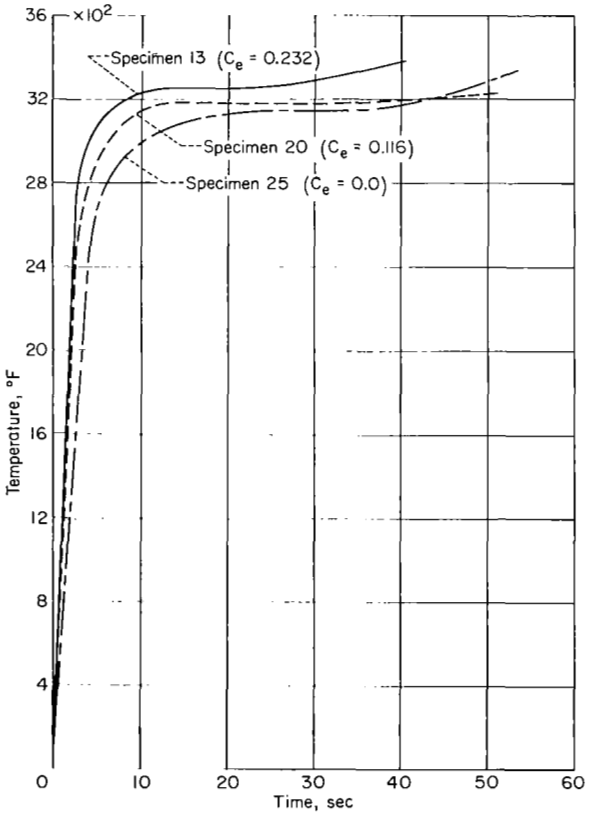

Figure 8.- Surface temperature histories for tests with 2-inch arc-jet nozzle.

Surface Energy Balance

The energy input at the surface of the test specimen must be accommodated by a combination of three mechanisms: reradiation from the surface, blocking of heat input by the gases transpired into the boundary layer, and conduction to the material behind the surface. In the tests reported herein, the heat input consisted of the convective heating plus the heating of the surface resulting from combustion of the char.

The heat inputs and the heat accommodated by each mechanism of energy are shown in table II for tests in nitrogen, in 11.6-percent oxygen, and in 23.2-percent oxygen. The tests were made with the 2-inch arc-jet nozzle. The measured cold-wall heating rate is reduced by a factor of 1/3 by the hot-wall correction. The combustive heating was calculated by using the assumptions that all the char which is removed reacts with oxygen to form carbon monoxide and that all the heat is absorbed by the surface. The reradiation component shown in table II was measured directly by the infrared radiometer which had been calibrated with a high-temperature black body.

TABLE II.- ENERGY-BALANCE TESTS WITH 2-INCH-DIAMETER NOZZLE

Specimen number	13	20	25
Gas composition, percent O_2	23.2(air)	11.6	0
Test time (measured), sec	15	15	30
Cold-wall heating rate (measured), Btu/ft^2-sec	175	175	174
Hot-wall heat input, Btu/ft^2-sec	116	116	116
Combustive heat input, Btu/ft^2-sec	35	25	0
Net heat input, Btu/ft^2-sec	151	141	116
Heat reradiated (measured), Btu/ft^2-sec	92	84	81
Heat blocked, Btu/ft^2-sec	10	7	3
Heat absorbed, Btu/ft^2-sec	58	42	16
Total heat accommodated, Btu/ft^2-sec	160	133	100

From tests of Teflon models it appears that the flow is turbulent with the 2-inch nozzle; therefore, the heat blocked was calculated by using a transpiration factor of 0.20. The heat absorbed includes the heat absorbed by the solid, the heat of pyrolysis, and the heat absorbed by the gaseous products of pyrolysis. It was assumed that 2,000 Btu/lb was required to raise the temperature of the phenolic nylon to the surface temperature.

For the tests in air and 11.6-percent oxygen, the difference between estimated heat input and estimated heat accommodated is approximately 6 percent. For the test in nitrogen, however, the estimated heat accommodated is about 14 percent lower than the estimated heat input. The error of 14 percent is consistent with the accuracy of the various measurements and assumptions used to prepare the table.

Material Effectiveness

A convenient parameter for evaluating the relative thermal performance of materials is defined as the total heat input to the surface before a temperature

rise of 300° F is experienced at the back surface divided by the weight of heat-shield material; that is,

$$E = Q/W$$

The results of these tests are shown in table III and the data are plotted in figure 9. When the oxygen concentration is near that of air, the effectiveness is not strongly influenced by oxygen concentration. The effectiveness increases with decreasing oxygen concentration particularly at low oxygen concentration. The effectiveness is more than 70 percent greater for tests conducted in nitrogen than for tests conducted in air.

TABLE III.- EFFECTIVENESS TESTS WITH 2-INCH-DIAMETER NOZZLE

Specimen	Percent O_2 in test gas	Specimen thickness, in.	Specimen density, lb/cu ft	$q_{c,o}$, Btu/ft^3-sec	Time for 300° F temperature rise	E, Btu/lb
1	23.2	0.7509	75.26	174	173	6,400
2	23.2	.7504	75.21	175	175	6,510
3	11.6	.7500	75.24	178	204.4	7,750
4	11.6	.7507	74.78	181.5	203	7,900
5	5.8	.7510	75.20	176	225.5	8,320
6	5.8	.7517	75.14	175	219	8,150
7	0	.7502	75.35	178	298	11,290
8	0	.7502	75.21	177	297	11,190

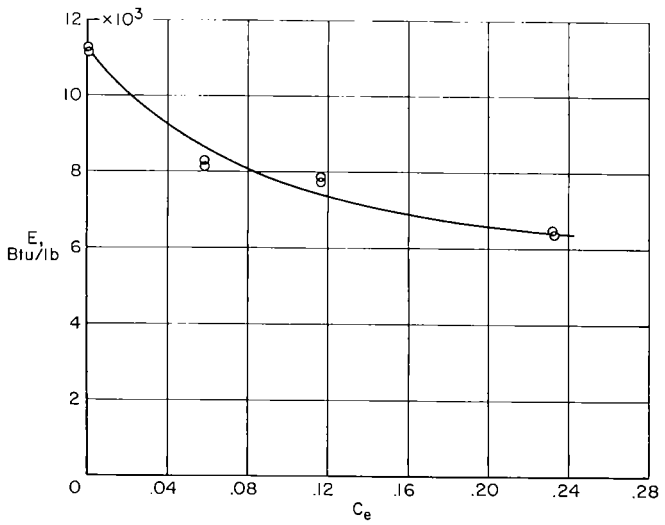

Figure 9.- Effect of oxygen concentration on thermal effectiveness of phenolic nylon. Tests with 2-inch nozzle.

DISCUSSION

Char Formation

Char is formed as one of the products of pyrolysis of a charring ablation material. When a material of this type, such as phenolic nylon, is exposed to heat, several distinct layers of material presumably corresponding to different degrees of thermal degradation can be identified.

The specimens shown in the photographs of figure 10 evidence these distinct layers of material. The specimen shown in figure 10(a) was tested in an arc-jet stream containing 5.8-percent oxygen and the specimen shown in figure 10(b) was tested in nitrogen. The following four layers can be observed in each photograph:

(1) A porous black layer which is easily identified as charred material

(2) A layer having a porous structure in which the nylon has apparently decomposed into gaseous products

(3) A nonporous layer in which the nylon has apparently melted

(4) A layer containing the remainder of the material in which no visible effects of heating can be detected

Separation frequently occurs between layers (1) and (2). (See fig. 10(b), for example.) This condition suggests that the phenolic resin is decomposing at this interface and that the material has little structural strength at this plane. The transition from layer (2) to layer (3) is abrupt as shown in both figures 10(a) and 10(b). The transition from layer (3) to layer (4) is less well defined.

The question arises as to which of the interfaces between different layers should be considered to be the depth to which pyrolysis has penetrated. In analyses of the performance of charring ablators during reentry heating, it is frequently assumed that all pyrolysis occurs at a single interface. On this basis, the most logical definition of an experimental pyrolysis interface is the one at which the largest percentage of pyrolysis occurs. Most of the nylon decomposes to yield gaseous products, whereas a large percentage of the phenolic remains as a solid in the form of char. Therefore, if the interpretation of the layers observed in figure 10 is correct, the pyrolysis interface should be defined as the interface between layers (2) and (3); that is, the pyrolysis interface separates the zone in which the nylon is melted from the zone in which it has decomposed. The measured values of depth of pyrolysis shown in table I are the distances from the original outer surface to the pyrolysis interface as defined previously. This pyrolysis interface which was clearly defined in all specimens tested also provides a good reference in experimental measurements.

Char Removal

To this point it has been established that in the low-enthalpy subsonic arc jet used in the present investigation, char removal does not occur without oxidation. With high oxygen content in the test stream and/or low heating rates, the char-removal process is reaction-rate controlled. With low oxygen concentrations and high heating rates, the process appears to be diffusion controlled. However, under certain conditions the rate of char removal is greater than that predicted on the basis of a diffusion controlled oxidation mechanism of char removal. Insufficient data are available to explain this result completely; however, a number of pertinent observations can be made.

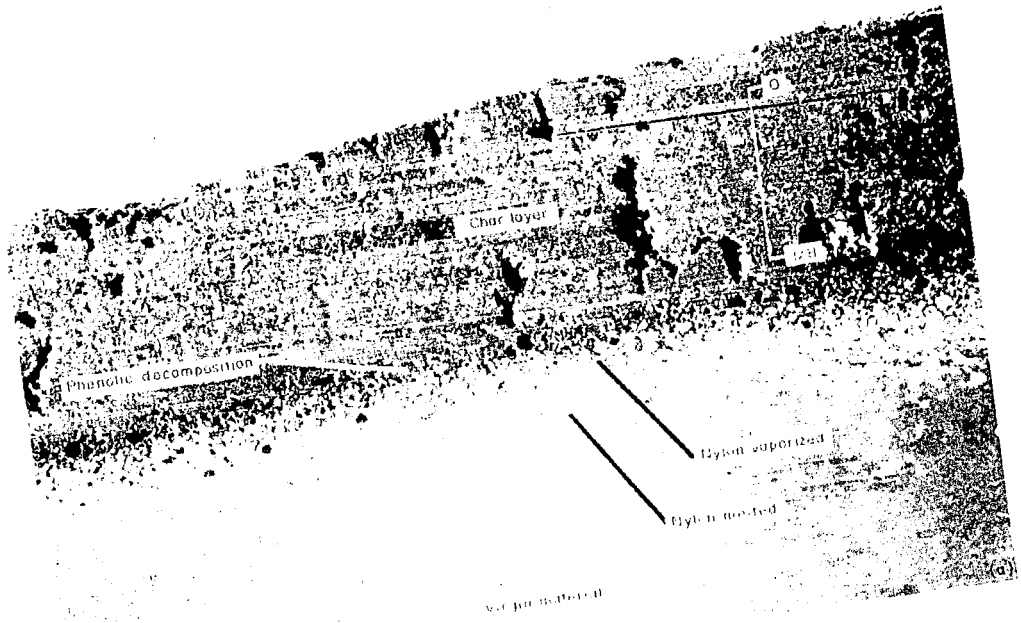

L-64-353

(a) Specimen tested in stream containing 5.8-percent oxygen and approximately 94.2-percent nitrogen.

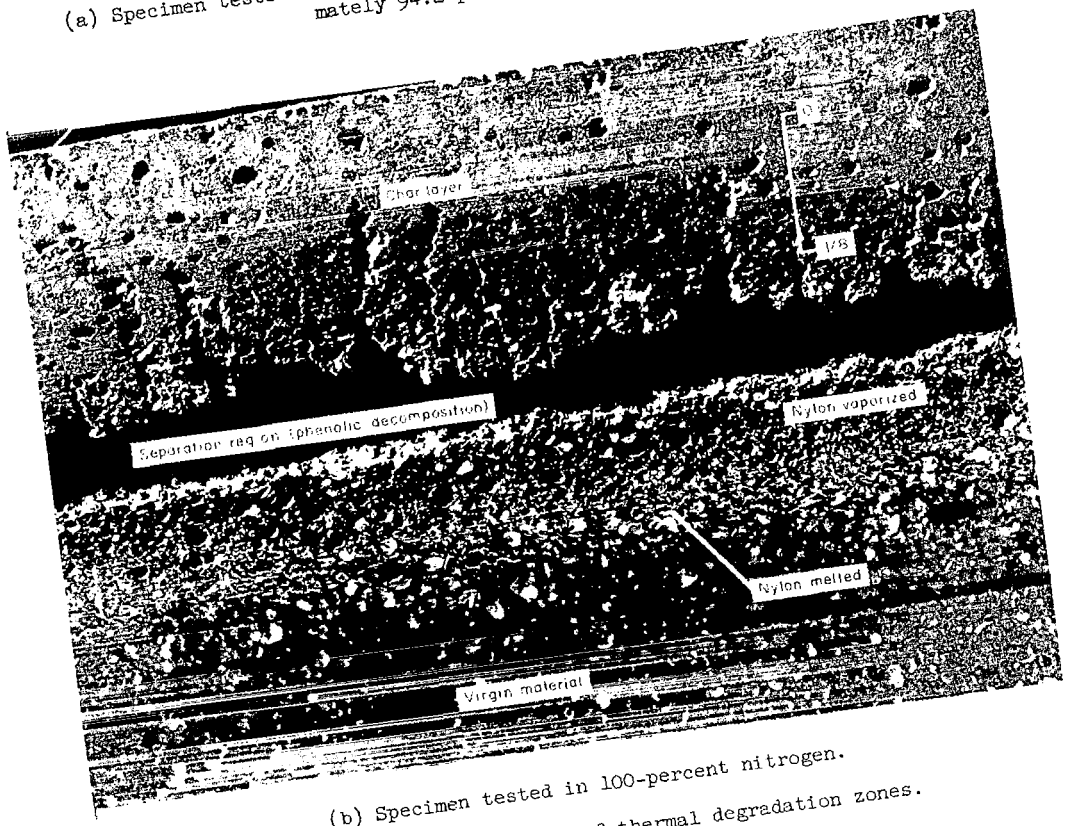

L-64-354

(b) Specimen tested in 100-percent nitrogen.

Figure 10.- Identification of thermal degradation zones.

Photographs of specimens tested in streams of different compositions are shown in figure 11. All the specimens were tested with the 2-inch-diameter nozzle for about 120 seconds. The surfaces of the specimens tested in a stream containing 50-percent oxygen (fig. 11(a), top view) present a uniform appearance from the center to the edge. This condition is in contrast to the specimens tested in streams of lesser oxygen content except for the specimen tested with no oxygen which experienced no char removal. Apparently, when the stream has low oxygen content, most of the oxygen is removed from the boundary layer when the flow impinges on the center portion of the specimen. However, with the higher oxygen concentration considerable oxygen remains in the boundary layer as it flows outward from the stagnation point and the edge of the specimen is oxidized in much the same manner as the center portion. This result further supports the conclusion reached earlier that the char removal is reaction-rate controlled with the higher oxygen concentration and diffusion controlled at lower oxygen concentrations.

Examination of the surfaces of the specimens shown in figures 11(b), 11(c), and 11(d) reveals an increasingly coarse grainlike structure as the oxygen content of the stream decreases. The surface of the specimen tested in nitrogen differs considerably from any of the others. This surface condition may be the limit to the trend exhibited in figures 11(b), 11(c), and 11(d). In addition to the grain pattern near the center of the specimens, considerable irregularity is observed near the edges of specimens shown in figures 11(b), 11(c), and 11(d).

The surface condition depends strongly on the test time. Specimens tested about 90 seconds are shown in figure 12. The formation of the grain pattern is barely evident at this time, even on the surface of the specimen tested in a stream containing only 11.6-percent oxygen. Specimens tested for 90 and 120 seconds in a stream containing 11.6-percent oxygen are shown in figure 13. The contrast between the surface conditions of these two specimens is obvious. A marked decrease in char thickness occurred between 90 and 120 seconds for specimens tested in a stream containing 11.6-percent oxygen. (See fig. 6(b).)

Because of the differences in the appearance of specimens tested for 90 seconds (fig. 12), the physical properties of the char may be different. The rate of char removal shown in figure 7 is based on changes in linear dimensions; therefore, a change in the density of the char would result in a change in the calculated rate of char removal. For chars similar to that shown in figure 13(b), the density was determined to be 11 percent less than that for other chars such as those shown in figure 13(a). This is a change in the average density of the char, and the change in density at the surface may be more or less than this amount. The lack of agreement between calculated and measured rates of char removal, which begins shortly after a test time of 90 seconds, may result from these changes in the character of the specimens.

Material Effectiveness

The relative ability of various materials to limit the back surface temperature rise when the front surface is exposed to a given environment has been used

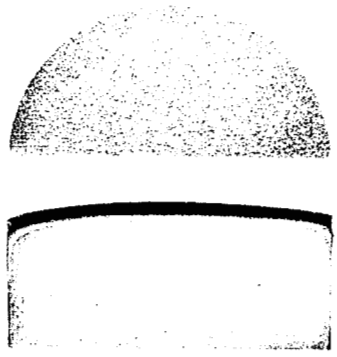

(a) C_e = 50 percent.

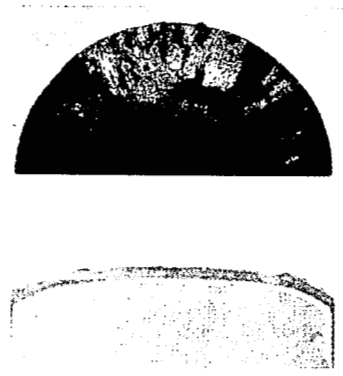

(b) C_e = 23.2 percent (air).

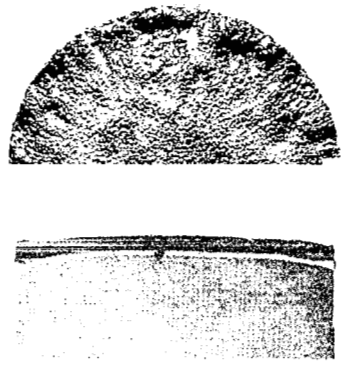

(c) C_e = 11.6 percent.

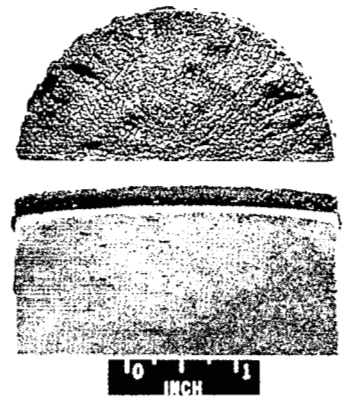

(d) C_e = 5.8 percent.

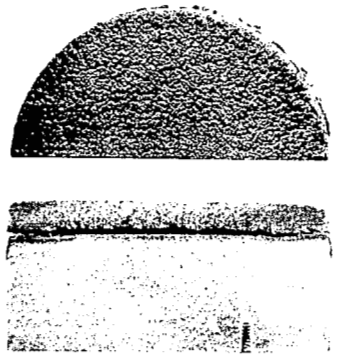

(e) C_e = 0 percent.

L-64-355

Figure 11.- Effects of stream composition on specimen physical characteristics for exposure times of 120 seconds or greater. Tests made with the 2-inch arc-jet nozzle.

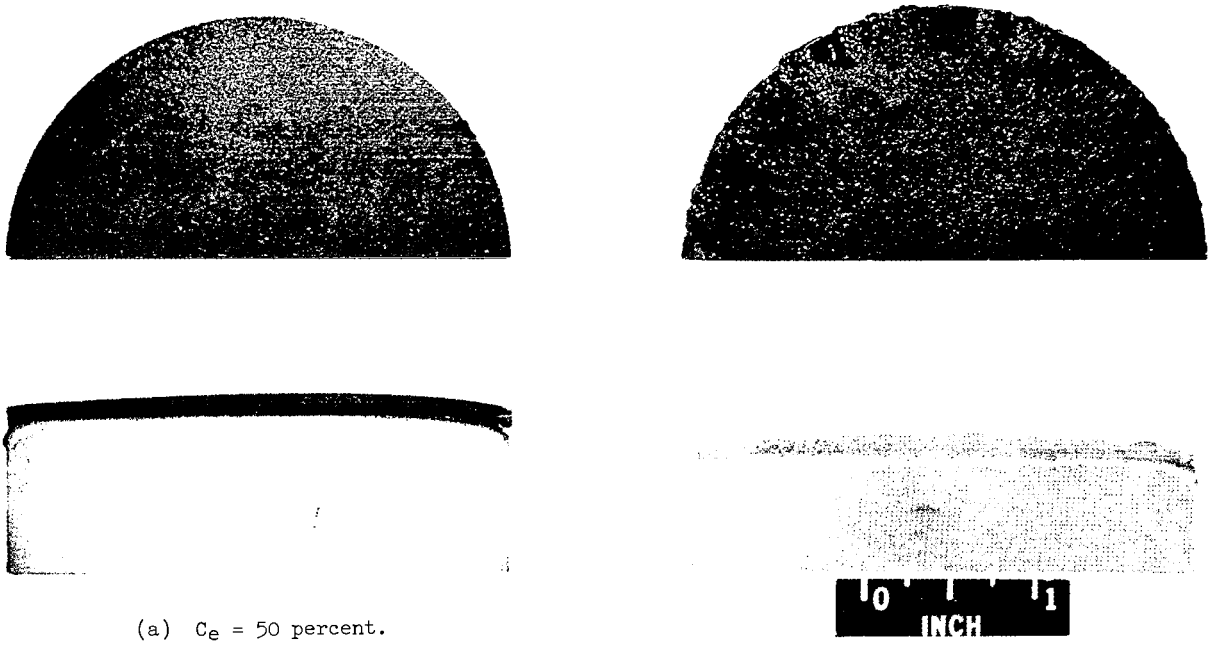

(a) C_e = 50 percent.

(b) C_e = 23.2 percent (air).

(c) C_e = 11.6 percent.

L-64-356

Figure 12.- Effects of stream composition on specimen physical characteristics for exposure times of about 90 seconds. Tests made with the 2-inch arc-jet nozzle.

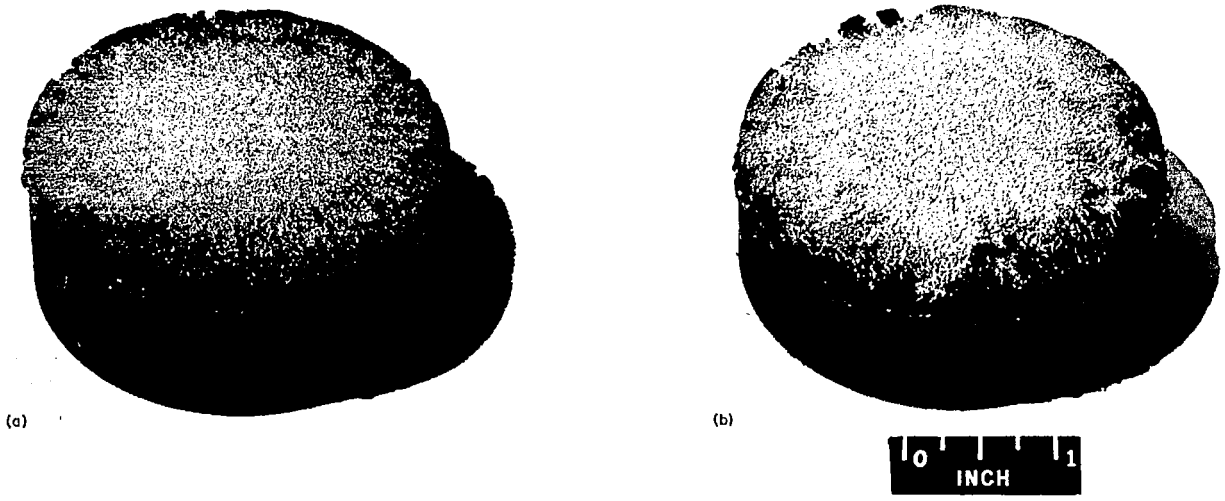

(a) 90 seconds. (b) 120 seconds. L-64-357

Figure 13.- Effect of exposure time on surface condition of specimens tested with the 2-inch arc-jet nozzle in a stream containing 11.6-percent oxygen.

in screening test programs to evaluate the effectiveness of different materials and to identify those materials which should be subjected to further study. (See ref. 1.) Considerable caution, however, must be exercised in interpreting the results of such tests. Results of tests of materials having surfaces which do not react chemically with the test stream (for example, glass surfaces) may be unaffected by the stream composition, whereas results of tests of materials having surfaces which oxidize will be strongly influenced by the concentration of oxygen in the test stream. Further, it is shown in reference 3 that in order to achieve simulation of performance at high reentry velocity in the test facility used in the present investigation, the oxygen concentration in the test stream should be between 0.03 and 0.05. The extent to which the performance of different classes of materials are affected by various environmental parameters must therefore be considered when the relative effectiveness of materials of different classes is evaluated, particularly when the test environment differs greatly from the flight environment in which the material is to be applied.

CONCLUDING REMARKS

Oxidation effects are a major factor in the performance of char-forming ablators such as phenolic nylon. Because of the differences in the dimensional characteristics of specimens tested in air and in nitrogen, it is concluded that

without oxidation there is no char removal by the gas stream of the arc-jet facility at the operating conditions used in this investigation.

At high heating rates and with low total heat input for short test times, the removal of char is a diffusion controlled process. At lower heating rates the oxidation rate depends on the reaction rate. Apparently, all the available oxygen reacts with the char. At longer test times the rate of char removal appears to be greater than can be accounted for on the basis of oxidation. However, measured rates of char removal were based on linear measurements of the surface location. The analysis used in the correlation of results is based on the weight of char removed, and it is difficult to determine the density of the char near the surface. Further investigation of the abrupt change in the rate of char removal in tests is recommended.

For tests in gas streams having high oxygen concentrations, the heat input to the surface resulting from combustion is a significant fraction of the total heat input. When this heat input is considered, a reasonable balance between heat input and heat accommodated by various mechanisms can be calculated.

The effectiveness of a charring ablator as measured by back surface temperature rise is strongly influenced by the oxygen concentration in the test stream. The effectiveness of phenolic nylon tested in nitrogen is more than 70 percent higher than the effectiveness of the same material tested in air.

Langley Research Center,
National Aeronautics and Space Administration,
Langley Station, Hampton, Va., November 12, 1963.

APPENDIX

ANALYSIS OF OXIDATION

The oxidation of carbon surfaces in hot airstreams has been extensively studied analytically. (See refs. 10 to 12.) It is found that at low surface temperatures the rate of oxidation of carbon is controlled by the reaction rates. However, at higher surface temperatures the process is diffusion controlled; that is, the rate of oxidation is limited by the quantity of oxygen diffusing to the surface through the boundary layer. For porous carbon surfaces, the temperature at which the process becomes diffusion controlled is lower than it is for nonporous surfaces.

The char layer that is formed when charring ablators are heated tends to be porous, as evidenced by the fact that the gaseous products of pyrolysis transpire through it. In addition, injection of these pyrolysis products into the boundary layer reduces the quantity of oxygen diffusing to the surface. Therefore, it is anticipated that the oxidation of the char surface will be diffusion controlled, even at relatively low temperatures.

The rate at which oxygen diffuses to the surface is determined from the boundary-layer equation for conservation of oxygen. This equation is (from ref. 13):

$$\rho' u \frac{\partial C}{\partial x} + \rho' v \frac{\partial C}{\partial y} = \frac{\partial}{\partial y}\left(\frac{\mu}{N_{Sc}} \frac{\partial C}{\partial y}\right) \tag{A1}$$

The energy equation can be expressed in the following form:

$$\rho' u \frac{\partial H}{\partial x} + \rho' v \frac{\partial H}{\partial y} = \frac{\partial}{\partial y}\left[\frac{\mu}{N_{Pr}} \frac{\partial H}{\partial y} + \frac{\mu}{2}\left(1 - \frac{1}{N_{Pr}}\right)\frac{\partial u^2}{\partial y}\right] \tag{A2}$$

Equations (A1) and (A2) are based on a nonreacting mixture of two gases having the same heat capacity. If $N_{Pr} = 1$ or if $\partial u^2/\partial y$ is small compared with $\partial H/\partial y$, which is valid at stagnation regions, equation (A2) may be expressed approximately as follows:

$$\rho' u \frac{\partial H}{\partial x} + \rho' v \frac{\partial H}{\partial y} = \frac{\partial}{\partial y}\left(\frac{\mu}{N_{Pr}} \frac{\partial H}{\partial y}\right) \tag{A3}$$

The maximum rate of diffusion of oxygen to the surface is obtained when the concentration of oxygen at the wall vanishes. The boundary conditions for equations (A1) and (A3) are:

$$\left.\begin{aligned} C &= 0 && (y = 0) \\ H &= H_w && (y = 0) \end{aligned}\right\} \tag{A4}$$

$$\left.\begin{aligned} C &\to C_e && (y = \infty) \\ H &\to H_e && (y = \infty) \end{aligned}\right\} \tag{A5}$$

The oxygen concentration and the enthalpy can be replaced by the dimensionless variables

$$\overline{C} = \frac{C}{C_e} \tag{A6a}$$

$$\overline{H} = \frac{H - H_w}{H_e - H_w} \tag{A6b}$$

In terms of these new variables, equations (A1), (A3), (A4), and (A5) are

$$\rho' u \frac{\partial \overline{C}}{\partial x} + \rho' v \frac{\partial \overline{C}}{\partial y} = \frac{\partial}{\partial y}\left(\frac{\mu}{N_{Sc}} \frac{\partial \overline{C}}{\partial y}\right) \tag{A7a}$$

$$\rho' u \frac{\partial \overline{H}}{\partial x} + \rho' v \frac{\partial \overline{H}}{\partial y} = \frac{\partial}{\partial y}\left(\frac{\mu}{N_{Pr}} \frac{\partial \overline{H}}{\partial y}\right) \tag{A7b}$$

$$\overline{C} = \overline{H} = 0 \qquad (y = 0) \tag{A7c}$$

$$\overline{C} = \overline{H} \to 1 \qquad (y = \infty) \tag{A7d}$$

Because of the formal similarity of equations (A7a) and (A7b) and their boundary conditions (A7c) and (A7d), if the solution of equation (A7b) is

$$\overline{H} = \varphi\left(x, y, N_{Pr}\right) \tag{A8a}$$

the solution of equation (A7a) is

$$\overline{C} = \varphi\left(x, y, N_{Sc}\right) \tag{A8b}$$

where φ is the same function in both cases. It is shown in reference 14 that $\varphi\left(x,y,N_{Pr}\right)$ can be expressed as

$$\varphi\left(x, y, N_{Pr}\right) = N_{Pr}^{0.4} \varphi_1(x, y) \tag{A8c}$$

Therefore,

$$\varphi\left(x,y,N_{Sc}\right) = N_{Sc}^{0.4}\varphi_1(x,y) \tag{A8d}$$

The rate at which oxygen diffuses to the wall is

$$\dot{m}(O_2) = C_e\left(\frac{\mu}{N_{Sc}}\frac{\partial\overline{C}}{\partial y}\right)_w \tag{A9a}$$

The aerodynamic heating rate is

$$q_c = \left(H_e - H_w\right)\left(\frac{\mu}{N_{Pr}}\frac{\partial\overline{H}}{\partial y}\right)_w \tag{A9b}$$

The ratio of rate of diffusion of oxygen to the surface to rate of heat transfer is

$$\frac{\dot{m}(O_2)}{q_c} = \frac{C_e}{H_e - H_w}\frac{\left(\frac{\mu}{N_{Sc}}\frac{\partial\overline{C}}{\partial y}\right)_w}{\left(\frac{\mu}{N_{Pr}}\frac{\partial\overline{H}}{\partial y}\right)_w} = \frac{C_e}{H_e - H_w}\frac{\left[\mu N_{Sc}^{-0.6}\frac{\partial\varphi_1(x,y)}{\partial y}\right]_w}{\left[\mu N_{Pr}^{-0.6}\frac{\partial\varphi_1(x,y)}{\partial y}\right]_w} = \frac{C_e}{H_e - H_w}N_{Le}^{0.6} \tag{A9c}$$

Therefore,

$$\dot{m}(O_2) = C_e N_{Le}^{0.6}\frac{q_c}{H_e - H_w} \tag{A10}$$

With $N_{Le} = 1$ and based on the assumption that the energy and concentration boundary-layer thicknesses are equal, this result can be applied to turbulent flow.

The convective heating rate that is obtained with mass injection can be expressed approximately in terms of the rate of injection and the convective heating rate with no injection as follows:

$$q_c = q_{c,o} - \eta\left(H_e - H_w\right)\left(\dot{m}_c + \dot{m}_p\right) \tag{A11}$$

Equation (A11) is based on a linear approximation of ablation theory. (See refs. 15 and 16.)

Char Removal

The rate of char removal is

$$\dot{m}_c = \lambda \dot{m}(O_2) \tag{A12}$$

where λ is the weight of char removed per unit weight of oxygen diffusing to the surface. It may be assumed that all the available oxygen reacts with the carbonaceous char. In reality, the products of pyrolysis are also available for reaction at the surface or in the boundary layer. The extent to which these products enter in the reaction processes can be determined analytically only by a detailed aerothermochemical analysis. These effects can be studied parametrically from the present analysis by adjusting the values of λ and Δh_1. For example, if the reaction at the surface is

$$2C + O_2 \rightarrow 2CO$$

and all the available oxygen reacts with the char, $\lambda = 3/4$. However, if only one-half of the available oxygen reacts with the char, $\lambda = 3/8$ instead of $3/4$. In the present analysis it has been assumed that all the available oxygen reacts with the char. From equations (A10), (A11), and (A12), the rate of char removal by oxidation is

$$\dot{m}_c = \frac{\lambda C_e N_{Le}^{0.6}}{1 + \lambda \eta C_e N_{Le}^{0.6}} \left(\frac{q_{c,o}}{H_e - H_w} - \eta \dot{m}_p \right) \tag{A13}$$

Combustive heating.- The oxidation of carbon is an exothermic process. For a surface reaction such as the one under consideration, it is anticipated that virtually all the heat generated by the reaction will be absorbed by the surface. This conclusion follows from the inability of the heat thus generated to flow to the higher temperature regions exterior to the surface. The combustive heating rate is

$$q_1 = \dot{m}_c \Delta h_1 \tag{A14}$$

where Δh_1 is the heat of combustion per unit weight of char.

Heat of Ablation

The significance of this heating can best be understood by determining its effect on the heat of ablation. The heat of ablation is defined as follows:

$$H_a = \frac{q_{c,o} + q_r}{\dot{m}} \tag{A15}$$

where q_r is net radiant heat input.

When the surface is subjected to high radiant heating rates $(q_r > 0)$, use of the linear approximation leads to considerable error and actual solutions of the boundary-layer equations must be used (ref. 17) rather than equation (A11). The surface of a charring ablator normally maintains a high temperature, and the net radiant heat input is negative. Therefore, equation (A11) is valid for charring ablators for most heating conditions. From an energy balance at the surface, the rate of mass injection is

$$\dot{m} = \frac{q_c + q_l + q_r}{\Delta h} \tag{A16}$$

Equations (A10), (A11), (A12), (A14), (A15), and (A16) can be combined to yield the following result:

$$\frac{H_a}{\Delta h} = \left(1 + \frac{q_r}{q_{c,o}}\right) \frac{1 + \dfrac{\eta(H_e - H_w)}{\Delta h} + \eta C_e N_{Le}^{0.6\lambda} \dfrac{\Delta h_l}{\Delta h}}{1 + C_e N_{Le}^{0.6\lambda} \dfrac{\Delta h_l}{\Delta h} \dfrac{\Delta h}{H_e - H_w} + \dfrac{q_r}{q_{c,o}}} \tag{A17}$$

In the absence of combustive heating, $q_l = 0$ and equation (A17) yields

$$\frac{H_a}{\Delta h} = 1 + \eta \frac{H_e - H_w}{\Delta h} \tag{A17a}$$

REFERENCES

1. Brooks, William A., Jr., Wadlin, Kenneth L., Swann, Robert T., and Peters, Roger W.: An Evaluation of Thermal Protection for Apollo. NASA TM X-613, 1961.

2. Scala, Sinclaire M., and Gilbert, Leon M.: Thermal Degradation of a Char-Forming Plastic During Hypersonic Flight. ARS Jour., vol. 32, no. 6, June 1962, pp. 917-924.

3. Swann, Robert T.: Approximate Analysis of the Performance of Char-Forming Ablators. NASA TR R-195, 1964.

4. Brooks, William A., Jr., Swann, Robert T., and Wadlin, Kenneth L.: Thermal Protection for Spacecraft Entering at Escape Velocity. [Preprint] 513F, Soc. Automotive Eng., Apr. 1962.

5. Chapman, Andrew J.: An Experimental Evaluation of Three Types of Thermal Protection Materials at Moderate Heating Rates and High Total Heat Loads. NASA TN D-1814, 1963.

6. Pearce, Willard J.: Plasma Jet Temperature Study. WADC Tech. Rep. 59-346, U.S. Air Force, Feb. 1960.

7. Peters, Roger W., and Wadlin, Kenneth L.: The Effect of Resin Composition and Fillers on the Performance of a Molded Charring Ablator. NASA TN D-2024, 1963.

8. Georgiev, Steven, Hidalgo, Henry, and Adams, Mac C.: On Ablation for the Recovery of Satellites. Res. Rep. 47 (Contract AF 04(647)-278), AVCO Res. Lab., Mar. 6, 1959.

9. Savin, Raymond C., Gloria, Hermilo R., and Dahms, Richard G.: Ablative Properties of Thermoplastics Under Conditions Simulating Atmosphere Entry of Ballistic Missiles. NASA TM X-397, 1960.

10. Scala, S. M., and Nolan, E. J.: Aerothermodynamic Feasibility of Graphite for Hypersonic Glide Vehicles. Re-Entry and Vehicle Design, Vol. IV of Ballistic Missile and Space Technology, Donald P. Le Galley, ed., Academic Press, Inc. (New York), c.1960, pp. 31-63.

11. Nolan, Edward J., and Scala, Sinclaire M.: Aerothermodynamic Behavior of Pyrolytic Graphite During Sustained Hypersonic Flight. ARS Jour., vol. 32, no. 1, Jan. 1962, pp. 26-35.

12. Moore, Jeffrey A., and Zlotnick, Martin: Combustion of Carbon in an Air Stream. ARS Jour., vol. 31, no. 10, Oct. 1961, pp. 1388-1397.

13. Cohen, Nathaniel B.: Relations Between Heat, Mass, and Momentum Transfer in Laminar and Turbulent Boundary Layers. RAD-2-TR-57-33, AVCO Res. and Advanced Dev. Div., Sept. 24, 1957. (Supersedes RAD-2-TM-57-58.)

14. Fay, J. A., and Riddell, F. R.: Theory of Stagnation Point Heat Transfer in Dissociated Air. Jour. Aero. Sci., vol. 25, no. 2, Feb. 1958, pp. 73-85, 121.

15. Roberts, Leonard: Mass Transfer Cooling Near the Stagnation Point. NASA TR R-8, 1959. (Supersedes NACA TN 4391.)

16. Roberts, Leonard: A Theoretical Study of Stagnation-Point Ablation. NASA TR R-9, 1959. (Supersedes NACA TN 4392.)

17. Swann, Robert T.: Effect of Thermal Radiation From a Hot Gas Layer on Heat of Ablation. Jour. Aerospace Sci. (Readers' Forum), vol. 28, no. 7, July 1961, pp. 582-583.